Revista Facultad de Ingeniería

Title: **Finite element analysis of the osseointegration process in compression osteosynthesis plates**

Authors: Carlos David Becerra-Gutiérrez and Mateo Escobar-Jaramillo

DOI: **10.17533/udea.redin.20251191**

To appear in: *Revista Facultad de Ingeniería Universidad de Antioquia*

Received: March 28, 2025
Accepted: November 13, 2025
Available Online: November 13, 2025

Revista Facultad de Ingeniería, Universidad de Antioquia, p. p. 511991 Nov. 2025
C. D. Becerra-Gutiérrez *et al*.; Revista Facultad de Ingeniería, Nov. 2025. Available: https://www.doi.org/10.17533/udea.redin.20251191

Finite element analysis of the osseointegration process in compression osteosynthesis plates

Análisis de elementos finitos del proceso de osteointegración en placas de osteosíntesis compresivas

Carlos David Becerra-Gutiérrez[1*] https://orcid.org/0009-0007-5844-2900 and Mateo Escobar-Jaramillo[1] https://orcid.org/0000-0003-4478-5439

[1]Ingeniería Biomédica, Universidad Autónoma de Bucaramanga. Avenida 42 # 48 – 11. C. P. Bucaramanga, Colombia

Corresponding author: Carlos David Becerra-Gutiérrez
E-mail: cbecerra566@unab.edu.co

KEYWORDS
Simulation techniques; Biomedical engineering; Research and experimental development
Ingeniería biomédica; Modelo de simulación; Investigación y desarrollo experimental

ABSTRACT
Musculoskeletal injuries are a leading cause of disability worldwide. Orthopedic surgery commonly employs osteosynthetic devices, such as compression plates, which require proper osseointegration for successful outcomes. Although titanium and its alloys are widely used for their mechanical strength and biocompatibility, limited osseointegration can result in clinical complications and require surgical reintervention. In this study, an integrated computational model combining finite element analysis in COMSOL with a biological module in MATLAB was developed to simulate the osseointegration process in titanium compression plates. The model enabled the assessment of how plate geometry and mechanical stress distribution directly influence cellular responses at the fracture site. Results revealed localized compressive stresses along the fracture line, with a maximum value of 140 MPa. This stress promoted bone formation by day 40, with complete consolidation occurring around day 100. These findings suggest that the proposed model can serve as a predictive tool for optimizing osteosynthesis material design and improving clinical outcomes, with applications in the development of next-generation implants.

RESUMEN
Las lesiones del sistema musculoesquelético son una de las principales causas de discapacidad a nivel mundial. Entre las opciones terapéuticas, la cirugía ortopédica utiliza dispositivos de osteosíntesis como las placas compresivas que requieren una correcta integración del implante con el hueso para su éxito. Aunque el titanio y sus aleaciones son materiales ampliamente usados por su resistencia mecánica y biocompatibilidad, con frecuencia presentan limitaciones en la osteointegración que pueden derivar en complicaciones clínicas y reintervenciones quirúrgicas. En este estudio se desarrolló un modelo

computacional integrado mediante análisis de elementos finitos en COMSOL acoplado a un módulo biológico en MATLAB para simular el proceso de osteointegración en placas compresivas de titanio. El modelo permitió identificar cómo la geometría de la placa y la distribución de esfuerzos mecánicos influyen directamente en la respuesta celular en el sitio de fractura. Los resultados mostraron una localización de esfuerzos compresivos en la línea de fractura, con un valor máximo de 140MPa. Este esfuerzo indujo la formación ósea alrededor del día 40 y completo su consolidación aproximadamente el día 100. Estos hallazgos demuestran que este tipo de modelos pueden ser una herramienta predictiva que contribuyen al diseño de material de osteosíntesis y a mejorar los resultados clínicos, con aplicabilidad en el desarrollo de implantes de próxima generación.

1. Introduction

Bone fractures are a leading cause of disability worldwide, with over 178 million cases reported each year, a number expected to rise due to population aging and increasingly active lifestyles [1] [2]. These injuries constitute a major medical challenge and a significant economic burden, generating substantial healthcare costs estimated at nearly USD 25.3 billion annually [3]. Approximately 5%–10% of cases require surgical intervention due to severity or complications during the healing process [4].

Compression plates remain the gold standard for treating complex fractures and improving patients' quality of life [4]. However, a major challenge is achieving adequate osseointegration while maintaining biomechanical stability at the fracture interface [5]. Although titanium alloys such as Ti-6Al-4V are the primary choice due to their high mechanical strength and biocompatibility, achieving complete integration between the implant and bone remains difficult. Implant loosening occurs in approximately 5%–15% of cases, often necessitating reintervention and increasing healthcare costs [6].

Recent studies have investigated the effects of fixation plates on bone healing. Research has established mechanical forces as key drivers of bone adaptation and remodeling, forming the biological basis for regeneration under load [7]. Building on this principle, finite element analysis (FEA) has been used to evaluate new plate designs for tibial fractures, demonstrating that plate geometry can affect stability and stress distribution [8]. Comparative studies of standard plates versus three-dimensional-printed titanium plates in acetabular fractures have further highlighted the potential of advanced manufacturing techniques to enhance fixation outcomes [9]. Similarly, analyses of different titanium plate configurations for scapular fractures have shown that plate shape and screw layout can produce notable differences in mechanical performance [10].

Despite these advancements, a clear knowledge gap remains. While most studies focus on plate mechanics or general bone response to loading, the specific influence of compression plates on cellular activity at the fracture site remains poorly understood. Integrating mechanical and biological models may offer deeper insight into bone–implant interactions, support the optimization of plate design, and help reduce complications, ultimately improving clinical outcomes worldwide.

This study aimed to develop and evaluate an integrated computational model that combines mechanical and biological processes to predict bone healing in fractures treated with compression plates. Using FEA in COMSOL, the model simulated interaction between a titanium implant and fractured bone, assessing how the forces generated by the screws and plate influence cellular behavior at the fracture site.

2. Methodology

2.1. Biological Mechanotransduction Model

The mathematical model used in this study describes the relationship between cellular behavior and mechanically induced stress, as previously reported [11] [12]. Briefly, bone cellular behavior was defined using a system of first-order differential equations that couple key factors involved in the osteosynthesis process, including signaling pathways (RANK, RANKL, and OPG) and cellular population and metabolic dynamics (osteocytes, osteoclasts, and osteoblasts). Additionally, the model incorporates equations representing the mechanical behavior of bone. This system is organized from **Equation 1** to **Equation 10**, as follows:

$$\sigma = \frac{F}{A}. \quad (1)$$

Here, mechanical stress (σ) is represented as a force (F) exerted over a specific area (A).

In **Equation 2,** k_{byp} represents the constant rate of osteocyte differentiation, and k_{yd} denotes the constant rate of osteocyte apoptosis. Furthermore, x_b and x_y correspond to the active osteoblast and osteocyte populations, respectively.

$$\frac{dx_y}{dt} = k_{byp}(x_b - X_{bss}) - k_{yd}(x_y - X_{yss}). \quad (2)$$

The stress magnitude F_{sti} (**Equation 3**) is required and depends on the osteocyte population. As shown in **Equation 3**, this force initiates the release of nitric oxide (NO) and Prostaglandin E (PGE) factors, both of which are essential mediators in the osteosynthesis process.

$$F_{sti} = \frac{F_s\, x_y}{(1+\exp(-(k_{Fs}\, F_s + k_y\, x_y)))}. \quad (3)$$

In **Equation 4**, F_S represents the mechanical stress applied to the model, where σ from **Equation 1** is substituted accordingly.

$$F_s = \frac{F_a}{A_B}. \quad (4)$$

In **Equation 5**, x_{no} represents the NO dynamics. This variable depends on a constant rate of NO release from osteocytes (k_{yno}), a degradation term with a constant rate (k_{nod}), and an external input (X_{nod}).

$$\frac{dx_{no}}{dt} = k_{yno}\, F_{sti} - k_{nod}\, x_{no} + x_{noe}. \quad (5)$$

Equation 6 results from the interaction between force stimuli and osteocytes. It is further influenced by the constant production of NO, represented by K_{nopge}, a degradation term (K_{pged}), and additional external inputs.

$$\frac{dx_{pge}}{dt} = k_{ypge}\, F_{sti} + k_{nopge}\, x_{no} - k_{pged}\, x_{pge} + x_{pgex}. \quad (6)$$

The osteoblast response (x_r) is described in **Equation 7**, which shows that PGE factors are involved in bone formation.

$$\frac{dx_r}{dt} = D_r\, \pi_c - \frac{D_B}{\pi_c} x_r + k_{pger}\, x_{pge}. \quad (7)$$

In **Equations 8** and **9**, the responding osteoblast (x_r) contributes to the osteoblast dynamics (x_b), while the osteoclast population (x_c) depends on different receptors regulated by the occupancy ratio of TGF-β receptors (Π_c).

$$\frac{dx_b}{dt} = \frac{D_B}{\pi_c} x_r - k_B x_b \quad (8)$$

$$\frac{dx_c}{dt} = D_c \pi_L - D_A \pi_c x_c \quad (9)$$

Finally, using the preceding equations, **Equation 10** was derived. This equation describes how the stress applied to a specific area modifies the activity of osteoclast (x_c), osteoblast (x_b), and osteocyte (x_y) populations, including growth and development rates, represented by k_{res} and k_{for}, respectively.

$$\frac{dr_B}{dt} = \frac{-k_{res}}{X_c} x_c + \frac{-k_{for}}{X_b} x_b + \frac{1}{X_y} x_y - k_{rB} r_B \quad (10)$$

Together, these equations form the mathematical framework for simulating the osteosynthesis process over a 365-day period. For clarity and reproducibility, the numerical values and units of all model parameters are summarized in **Table 1** [7][11][12].

Table 1. Numerical values of parameters (adapted from [7][11][12])

Parameter	Symbol	Value
Induced force	F	500 N
Cross-sectional area	A	$2e^{-4}$ m^2
Osteoclast activation rate	D_C	$1e^{-3}$
Osteoclast apoptosis rate	D_a	0.1
Osteoblast formation rate	D_B	$1e^{-4}$
Osteoblast apoptosis rate	k_B	1
Osteocyte differentiation rate	k_{byp}	0.1
Osteocyte apoptosis rate	k_{yd}	1
RANKL occupancy factor	Π_L	0.02
Receptor occupancy factor	Π_C	0.02
Osteoblast density	X_B	0.07
Osteoclast density	X_C	0.03
Osteocyte density	x_{yss}	$7.3e^{-3}$
Active osteocyte population	X_Y	0.6
Rate of RANKL formation	k_{for}	0.07
Coefficient of the RANK receptor to RANKL	k_{rb}	0.02
Resorption rate induced by osteoclasts	k_{res}	0.04

Steady-state reference value of osteoblasts	X_{bss}	$7.28e^{-4}$
Activation of osteoclasts induced by RANKL	k_y	1
RANKL signaling sensitivity factor	k_{Fs}	1
Expression coefficient of RANKL	k_{ypge}	$1e^{2}$
Basal expression level of RANKL	x_{pgex}	0
Inhibition constant by OPG	k_{nopge}	1
Basal level of OPG	x_{no}	0.3
Degradation constant of RANKL	k_{pged}	$1e^{2}$
Inhibition constant of OPG	k_{pger}	$1e^{-4}$
Proportionality factor between active and responding osteoblasts	D_r	0.02

2.2. Mechanical Model

To simplify the simulation, bone was modeled as an isotropic, linear elastic material under two key assumptions: (1) the induced forces on the bone are directly proportional to the applied force magnitude, and (2) the deformation response is uniform across all surfaces [7].

The computational model comprised the bone structure, an osteosynthesis plate, and two fixation screws. A geometrically simplified representation was used to evaluate the mechanical response of the bone–implant system while maintaining the proportional dimensions of each component [13]. The model was constructed and analyzed using COMSOL Multiphysics 5.5. **Figure 1** illustrates the modeled geometry, depicting the clinical scenario with the fracture site, the compression plate and screws, and the region selected for finite element simulation.

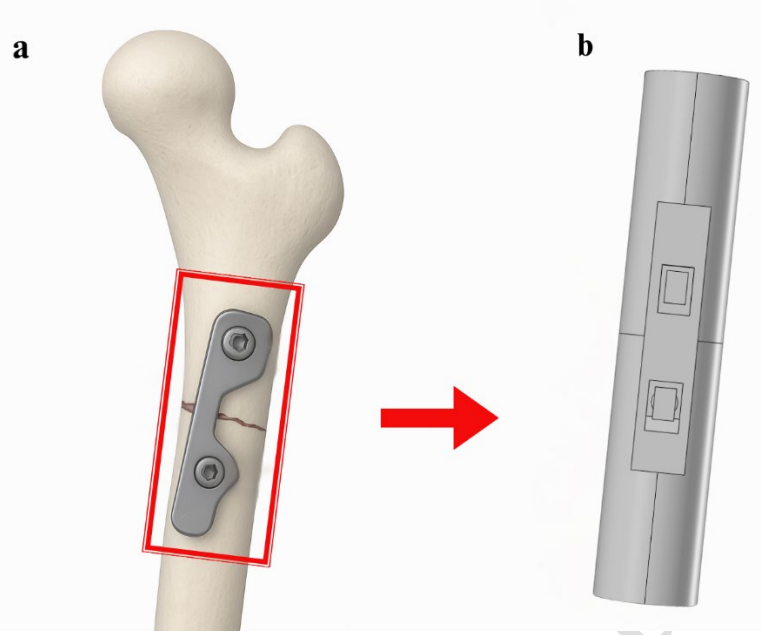

Figure 1. Representation of the simulated process: (a) clinical scenario of a transverse fracture stabilized with a compression plate and screws; (b) simplified computational model employed for FEA.

The bone was modeled as a long bone by extruding a cylindrical structure 4 cm in diameter and 20 cm in length. A transverse fracture was simulated by bisecting the cylinder and introducing a 0.1 mm gap between the two bone segments, as illustrated in the final model (**Figure 2a**).

For the compression plate, a rectangular surface was created at half the length of the bone and positioned symmetrically at the fracture midpoint. The plate was designed to conform to the bone surface and included two countersunk holes on its upper face for fixation screws (**Figure 2b**).

One of the holes had a standard fit for the screw size, while the other featured a countersunk compartment with a 35° positive inclination, slightly shifted to the left of the original screw position (**Figure 2c**). This modification was necessary to induce compressive stress at the fracture surface, ensuring that both bone segments align once the screws are placed [14].

The screws were modeled with a rectangular head and a pointed tip, measuring 2.4 cm in total length, 1.2 cm in maximum width, and 0.35 cm in body diameter [14] (**Figure 2d**).

The fully assembled model is presented in **Figure 2e**.

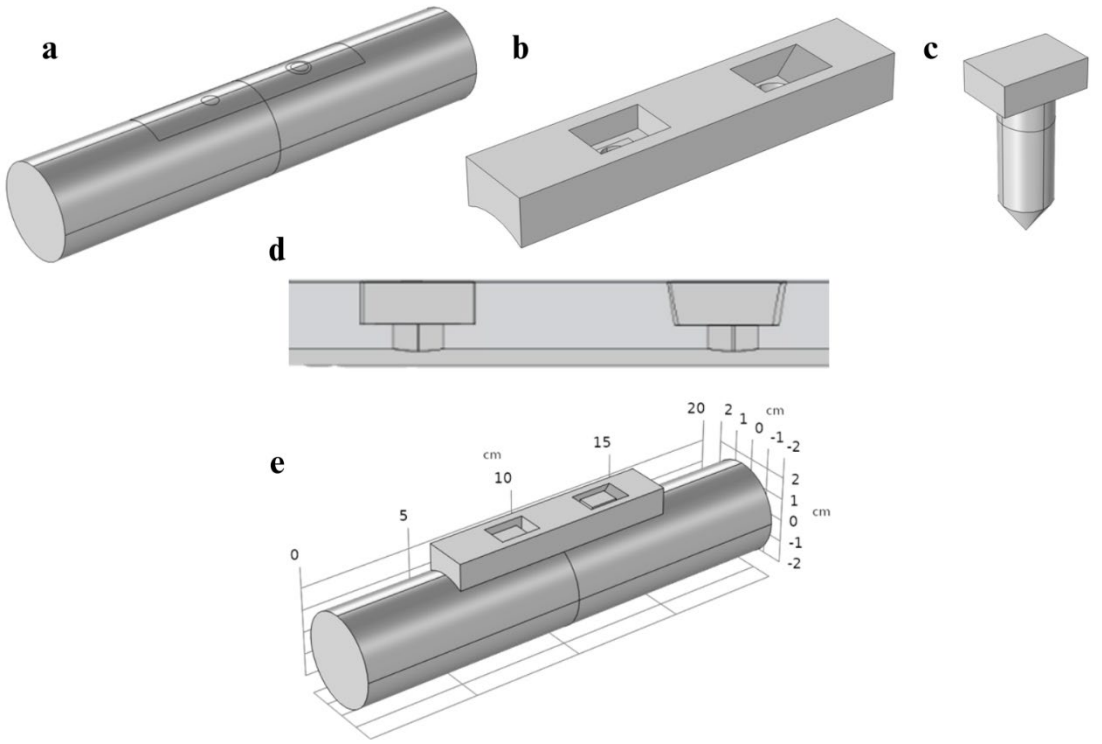

Figure 2. Geometrical modeling of the osteosynthesis system: (a) bone geometry, (b) compression plate geometry, (c) screw geometry, (d) screw countersink, and (e) assembled bone–plate model.

2.3. Finite Element Analysis Conditions

Before running the simulation, the parameters and boundary conditions of the entire model were defined to ensure proper behavior of each component.

Specific materials and their corresponding mechanical properties were assigned. Both the fixation screws and the osteocompressive plate were modeled using the titanium alloy Ti-6Al-4V, one of the most widely used materials in orthopedic implants [15].

For the bone, a custom material was defined. The material properties used in the simulation are summarized in **Table 2** [15][16].

Table 2. Material properties (adapted from [15][16])

Material	Young's Modulus	Poisson's Coefficient	Density
Bone	18 GPa	0.62	1908 kg/m^3

Titanium 6Al-4V	114 GPa	0.342	4430 kg/m^3

Fixation points were defined to ensure accurate bone interpretation and correct force application surfaces, enabling proper bone–implant interaction [17].

For this purpose, a longitudinal force was applied over the displaced fixation screw (**Figure 3**), while the opposite bone surface was constrained as a fixation point (**Figure 4**). This configuration induced a relative displacement between the two bone segments, producing mechanical stress at the fracture surface [17].

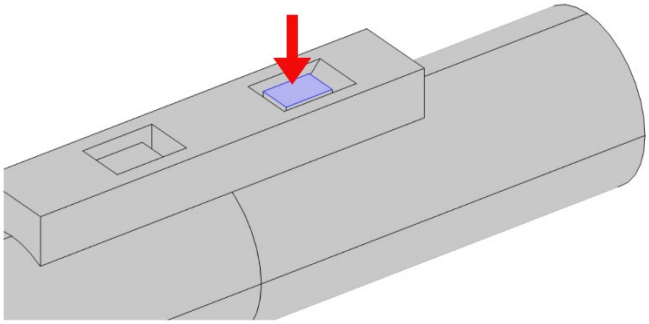

Figure 3. Force application surface

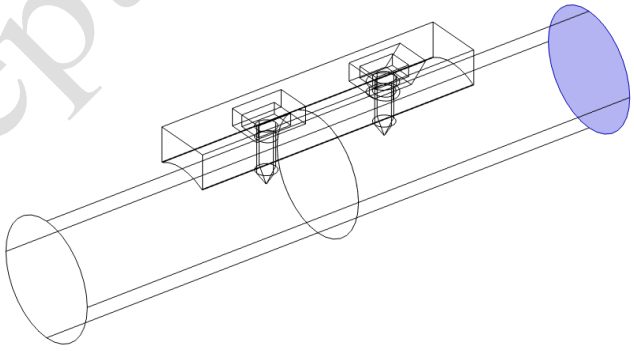

Figure 4. Clamping surface

The mesh was generated using tetrahedral elements, with a minimum element size of 0.08 cm and a maximum size of approximately 1.1 cm. Mesh elements included a maximum growth rate of 1.4, a curvature factor of 0.4, and a narrow region resolution of 0.7.

2.4 Model Implementation

To integrate both models, two complementary domains were established. COMSOL Multiphysics 5.5 was used to perform FEA of mechanical stress distribution at the bone–implant interface, whereas MATLAB/Simulink 2023a was used to implement the biological module describing osteoblast, osteoclast, and osteocyte activity. Coupling between the two environments was achieved through the exchange of boundary conditions and numerical outputs, enabling the integration of mechanical and cellular processes within a single predictive framework.

This integration strategy is illustrated in **Figure 5**, which shows the workflow connecting finite element outputs from COMSOL to biological simulations conducted in MATLAB.

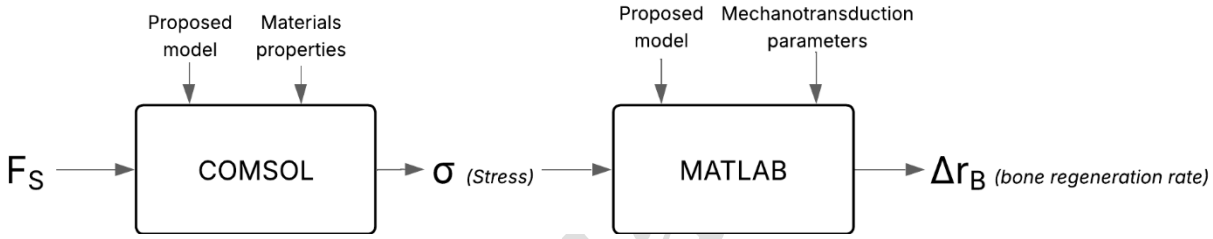

Figure 5. Integration of COMSOL and MATLAB: stress distribution (σ) obtained from FEA is coupled with a mathematical model to predict bone regeneration (Δr_B)

3. Results

The first simulation involved a nonlinear, stationary study using the von Mises criterion to analyze the applied stresses and the model's response to an initial force applied to the leading screw, thereby simulating the system's real behavior [18]. The resulting stress distribution was visualized using a color scale, where blue areas indicate minimal stress and orange to red areas represent high stress concentrations. **Figure 6** shows the stress distribution on the external surface of the model, whereas **Figure 7** illustrates the internal stress patterns within the bone boundaries, particularly at the fracture site [18].

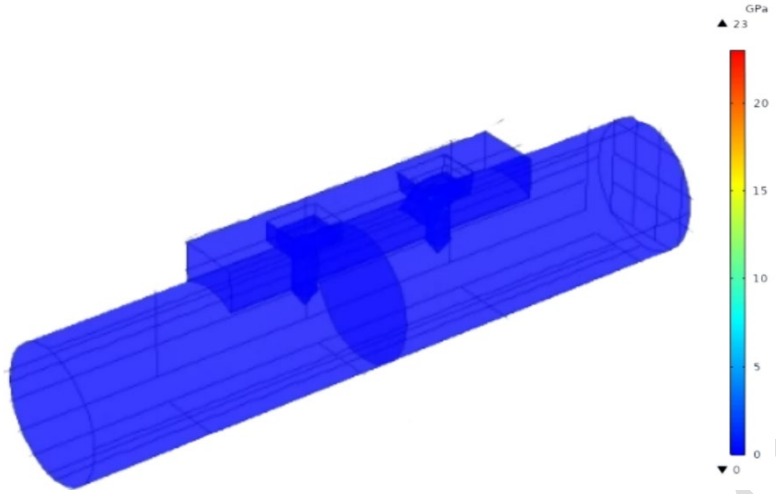

Figure 6. Mechanical stress distribution on the surface

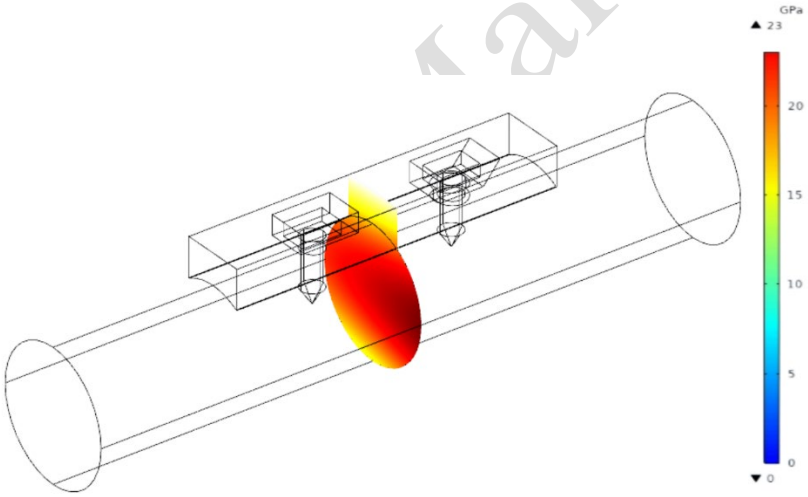

Figure 7. Mechanical stress distribution at the interface

The second simulation involved a time-dependent analysis conducted in MATLAB. The results of this analysis are presented in **Figure 8**.

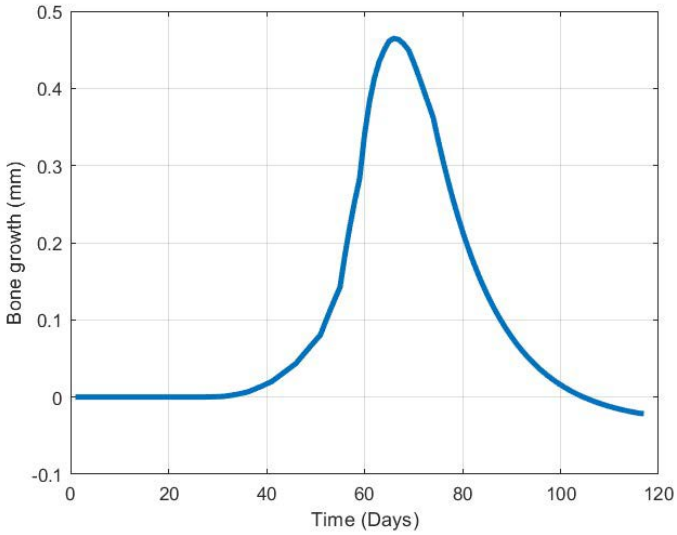

Figure 8. Osteosynthesis process induced by compressive plates at the bone–implant interface

The nonlinear stationary study demonstrated the expected behavior of the bone–implant model [18]. Stress concentrations were specifically observed on the internal bone surfaces, whereas the external bone surface and the implant showed minimal stress distribution, as indicated by the blue regions. Conversely, the fracture interface exhibited high stress levels, represented by the red and orange regions.

The FEA confirmed that the eccentric screw position and the inclined countersink of the compression plate generated localized compressive stress at the fracture site. This mechanical condition is crucial for fracture stabilization and bone healing, consistent with previous studies demonstrating that plate geometry and working length significantly influence fixation outcomes [19]. Notably, the compressive effect extended across the fracture gap—not only at the plate–bone interface—highlighting its clinical relevance.

When coupled with the biological module, the model replicated the characteristic three-phase pattern of bone healing: an initial rise in activity proportional to new bone formation, a peak phase of maximum cellular response, and a gradual return to baseline levels [20]. The simulation indicated early bone synthesis around day 40, with 0.4–0.5 mm of tissue filling the fracture gap, and complete consolidation by approximately day 100. These findings align with mechanobiological models linking stress magnitude to osteoblast and osteoclast regulation through pathways such as NO, PGE2, and RANK–RANKL–OPG [21] and are consistent with recent computational studies that couple FEA with cell differentiation algorithms [20].

The innovation of this study lies in integrating mechanical and biological processes within a single predictive framework. Although alternative materials, including metamaterial-structured plates [22] and bioactive PEEK scaffolds [21], offer benefits in reducing stress shielding or improving osteoinduction, Ti-6Al-4V remains superior in mechanical strength and clinical reliability. The present model demonstrates how implant mechanics directly influence biological cascades leading to osseointegration.

Furthermore, the observed compression levels fall within the optimal range for promoting healing while minimizing stress shielding [23], highlighting that the proposed model is mechanically efficient and biologically favorable [24].

Notably, the model used a simplified geometry using a cylindrical bone shaft with a clean transverse fracture and an idealized plate–screw configuration. In vivo factors, including anisotropic bone behavior, vascularization, cyclic physiological loading, and micromotion at the implant–bone interface, were not included. These simplifications were necessary to ensure computational feasibility. However, future work will incorporate more realistic geometries and biological processes.

4. Conclusion

In this study, we integrated mechanical and biological computational models to predict bone healing in transverse fractures stabilized with compression plates. Mechanically, the model confirmed that screw eccentricity and angled countersinks generate effective interfragmentary compression, providing stability while minimizing stress concentrations in the bone structure. Biologically, the translation of stress into cellular responses reproduced realistic healing dynamics, with new bone formation around day 40 and consolidation by approximately day 100, confirming implant-induced loading as a key driver of tissue regeneration.

The strength of this approach lies in its integration of mechanical stability and biological activity within a single predictive framework. This method evaluates how implant geometry and material influence osseointegration and also highlights the compressive effect as a clinically relevant advantage, reducing fragment displacement and optimizing conditions for fracture consolidation. Compared with studies that focus solely on structural mechanics or material innovations, this model offers a more comprehensive perspective bridging engineering and biology. It thus provides a foundation for developing personalized, next-generation orthopedic implants that enhance both biomechanical performance and clinical healing outcomes.

Declaration of competing interests

The authors declare that no competing interests—financial, professional, or personal—influenced the work presented in this manuscript.

Acknowledgment

The authors acknowledge the Universidad Autónoma de Bucaramanga (UNAB) and the Undergraduate Research Group “SIIBEC” for their support.

Funding

The Universidad Autónoma de Bucaramanga and the Program of Biomedical Engineering at UNAB supported this work.

Author contributions

C. D. Becerra-Gutierrez: Conducted the investigations, designed the methodology, validated the results, contributed to visualization, wrote the manuscript, and participated in its review and editing. M. Escobar-Jaramillo secured funding, managed the project, designed the methodology

5. Data availability statement

The authors confirm that the data supporting the results of this study are included within the article and/or its supplementary materials.

References

[1] International Osteoporosis Foundation, "Annual report 2023," 2023. [Online]. Available: https://www.osteoporosis.foundation/annual-report-2023

[2] Q. A. Meslier and S. J. Shefelbine, "Using finite element modeling in bone mechanoadaptation," Curr. Osteoporos. Rep., vol. 21, no. 2, pp. 105–116, 2023, doi: 10.1007/s11914-023-00776-9.

[3] M. Ceddia, G. Solarino, M. Tucci, L. Lamberti, and B. Trentadue, "Stress analysis of tibial bone using three different materials for bone fixation plates," J. Compos. Sci., vol. 8, no. 9, p. 334, 2024, doi: 10.3390/jcs8090334.

[4] Sociedad Española de Cirugía Ortopédica y Traumatología (SECOT), "Tratamiento quirúrgico de las fracturas de cadera," Manual del residente, 2021. [Online]. Available: https://unitia.secot.es/web/manual_residente/CAPITULO%2018.pdf

[5] N. Vilabrú Pagès and M. Baraldés Canal, "Osteosíntesis en el tratamiento de las fracturas: placas," in Manual del Residente, L. Marull Serra, Coord., Hospital Universitario "Doctor Josep Trueta" de Girona, 2021. [Online]. Available: https://unitia.secot.es/web/manual_residente/CAPITULO%2018.pdf

[6] F. G. Dittlar, "Lesiones óseas. Fracturas," in Lo esencial en ortopedia y traumatología, O. A. Romano and C. A. Fernandez, Eds., Fac. Cs. Médicas, UNLP, La Plata, Argentina, 2021, ch. 13, pp. 207–220. [Online]. Available: https://sedici.unlp.edu.ar/handle/10915/177962

[7] D. A. Garzón-Alvarado, C. A. Duque-Daza, J. J. Vaca-González, E. Barbosa Las Casas, D. L. Linero, G. de Boer, R. Das, and S. Ramtani, "Computational model of bone remodeling integrating osteocyte mechanotransduction and microdamage-driven self-repair," Acta Biomater, accepted 8 Sep. 2025, doi: 10.1109/IEMBS.2006.260532 (Author version)

[8] Z. Yan, C. Zou, G. R. Kenmegne, X. Pan, N. Ghimire, K. M. N. Silva, and Y. Fang, "Newly designed plate for the treatment of posterolateral tibial plateau fractures: a finite element analysis," J. Orthop. Surg. Res., vol. 19, no. 201, pp. 1–11, 2024, doi: 10.1186/s13018-024-04686-z.

[9] G. Lv, X. Chen, H. Wu, G. Wu, Y. Huang, and G. Huang, "Finite element analysis of the use of two new types of internal fixation for acetabular fractures," J. Orthop. Surg. Res., vol. 18, no. 841, pp. 1–13, 2023, doi: 10.1186/s13018-023-04337-9.

[10] Y. Shang, Y. Bi, Y. Cao, and Y. Wang, "Finite element analysis of titanium anatomic plate and titanium reconstructive plate for treatment of extra-articular fractures of the scapula," J. Orthop. Surg. Res., vol. 18, no. 134, pp. 1–10, 2023, doi: 10.1186/s13018-023-03614-x.

[11] S. Maldonado, S. Borchers, R. Findeisen, and F. Allgower, "Mathematical modeling and analysis of force induced bone growth," in 2006 International Conference of the IEEE Engineering in Medicine and Biology Society, New York, NY, USA, 2006, pp. 3154–3157, doi: 10.1109/IEMBS.2006.260532.

[12] L. Liu, Q. Shi, Q. Chen, and Z. Li, "Mathematical modeling of bone in-growth into undegradable porous periodic scaffolds under mechanical stimulus," J. Tissue Eng., vol. 10, 2019, Art. no. 2041731419827167, doi:10.1177/2041731419827167

[13] M. Doblaré, J. M. García, and M. J. Gómez, "Modelling bone tissue fracture and healing: A review," Eng. Fract. Mech., vol. 71, no. 13–14, pp. 1809–1840, 2004, doi: 10.1016/j.engfracmech.2003.08.003.

[14] P. Liokatis, G. Tzortzinis, C. P. Cornelius, Y. Malenova, K. T. Obermeier, and W. Smolka, "A finite element analysis of the trapezoidal plate. How to get a stable fixation at different fracture lines?," Injury, vol. 55, no. 12, Art. no. 112020, Dec. 2024, doi: 10.1016/j.injury.2024.112020.

[15] AM Material, "Introduction to Ti-6Al-4V titanium alloy," AM Material. [Online]. Available: https://am-material.com/es/news/introduction-to-ti-6al-4v-titanium-alloy/

[16] E. F. Morgan, G. U. Unnikrishnan, and A. I. Hussein, "Bone mechanical properties in healthy and diseased states," Annu. Rev. Biomed. Eng., vol. 20, pp. 119–143, 2018, doi: 10.1146/annurev-bioeng-062117-121139.

[17] P. Liokatis, G. Tzortzinis, C. P. Cornelius, Y. Malenova, K. T. Obermeier, and W. Smolka, "A finite element analysis of the trapezoidal plate. How to get a stable fixation at different fracture lines?," Injury, vol. 55, no. 12, Art. no. 112020, Dec. 2024, doi: 10.1016/j.injury.2024.112020

[18] Y. Li, P. Yi, Z. Zou, F. Lu, X. Zhang, and J. Zhang, "Finite element model with realistic bone geometries for the optimal design of internal fixation during the fibula healing process," Proc. Inst. Mech. Eng. H, vol. 238, no. 2, pp. 207–218, 2024, doi: 10.1177/09544119231221193.

[19] Y. Li, P. Yi, Z. Zou, F. Lu, X. Zhang, and J. Zhang, "Finite element model with realistic bone geometries for the optimal design of internal fixation during the fibula healing process," Proc. Inst. Mech. Eng. H, vol. 238, no. 2, pp. 207–218, 2024, doi: 10.1177/09544119231221193.

[20] L. Yan, J. L. Lim, J. W. Lee, C. S. H. Tia, G. K. O'Neill, and D. Y. R. Chong, "Finite element analysis of bone and implant stresses for customized 3D-printed orthopaedic implants in fracture fixation," Med. Biol. Eng. Comput., vol. 58, no. 5, pp. 921–931, 2020, doi:10.1007/s11517-019-02104-9.

[21] W. Zhang, D. Shi, S. Huang, S. Li, M. Zeng, and Y. Wei, "Personalized 3D-printed bioactive PEEK bone plate scaffold for treating femoral defects," RSC Adv., vol. 15, pp. 5060–5072, 2025, doi: 10.1039/d4ra07573k.

[22] H. C. Liu, Y.-H. Chan, S.-F. Huang, W.-C. Tsai, Y. Cheng, and C.-L. Lin, "Early stage prediction of bone regeneration using FEA and cell differentiation algorithms with 3D-printed PLA and PCL scaffolds: modeling and application to dorsal double-plating in distal radius fractures," 3D Print. Med., vol. 11, no. 1, Article 30, 2025, doi:10.1186/s41205-025-00278-7

[23] G. Zhang, J. Li, C. Shangguan, X. Zhou, Y. Zhou, and A. Huang, "A metamaterial bone plate for biofixation based on 3D printing technology," Int. J. Bioprinting, vol. 10, no. 4, p. 2388, 2024, doi: 10.36922/ijb.2388.

[24] Q. Wang, Y. Lin, and F. Chen, "Recent advances in 3D printing of biodegradable metals for orthopedic applications," J. Biol. Eng., vol. 17, no. 1, p. 56, 2023, doi: 10.1186/s13036-023-00371-7.